EFFECTIVE LOW-DIMENSIONAL POLYNOMIAL EQUATIONS
FOR BOSE-EINSTEIN CONDENSATES

ALEXANDRU I. NICOLIN[1,*], MIHAELA C. RAPORTARU[1], ANTUN BALAŽ[2]

[1]Department of Computational Physics and Information Technologies,
Horia Hulubei National Institute of Physics and Nuclear Engineering (IFIN-HH),
P. O. Box MG-6, 077125, Romania
[2]Scientific Computing Laboratory, Institute of Physics Belgrade, University of Belgrade,
Pregrevica 118, 11080 Belgrade, Serbia
*Corresponding author *E-mail*: alexandru.nicolin@nipne.ro

Abstract. In the first part of this article we briefly overview the fundamentals of Bose-Einstein condensation and survey a series of results concerning the effective equations which describe the dynamics of elongated and oblate Bose-Einstein condensates. In the second part of the paper we show how one can construct effective one- and two-dimensional polynomial Schrödinger equations which describe the longitudinal (transversal) dynamics of high-density cigar-shaped (pancake-shaped) Bose-Einstein condensates. These equations do not account for the interplay between the radial and the transversal modes of the condensate, but can accurately describe the dynamics of effectively longitudinal (transversal) nonlinear waveforms through the rescaled effective nonlinearity in the case of cigar-shaped (pancake-shaped) condensates.

1. INTRODUCTION

The first achievement of atomic Bose-Einstein condensation in 1995, in the groups of W. Ketterle from Massachusetts Institute of Technology and C. E. Wieman and E. A. Cornell from University of Colorado at Boulder, who were later awarded the 2001 Nobel Prize in Physics, paved the way for an unprecedented series of theoretical, computational and experimental investigations (see the textbook treatment of the subject in Refs. [1–3] and the general reviews and Nobel Lectures in Refs. [4–9]). Much of theoretical and computational research into Bose-Einstein condensates (BECs) uses the so-called Gross-Pitaevskii equation (GPE) to describe the dynamics of the condensate at (or very close to) $T = 0$ K. While the GPE was introduced to the community in the early sixties in two fundamental papers of Gross and Pitaevskii [10, 11], mathematically similar equations of physically different problems have been investigated long before that. The Ginzburg-Landau theory, for instance, was used in the early fifties to model superconductivity and, while physically unrelated to BECs, it gives rise to similar nonlinear equations. The same holds for the theory of quasi-monochromatic wave trains propagating in a weakly nonlinear dielectric (*e.g.*, a Kerr medium, where the dielectric constant depends on the square of the electric field), the weakly nonlinear dynamics of a wave train propagating at the surface of a liquid

(the so-called water-wave problem), the Langmuir oscillations (also referred to as Langmuir waves or electron plasma waves) that arise in non-magnetized or weakly magnetized plasmas, the Alfvén waves that propagate along an ambient magnetic field in a quasi-neutral plasma, etc. (see Ref. [12] for a review).

As the backbone of all these equation is the cubic nonlinearity, the investigations into nonlinear waveforms have been a recurrent research topic of continual interest, as can be seen from the BEC-focused reviews in Refs. [13–15], from the reviews on optical solitons in two- and three-dimensional physical settings (including spatiotemporal optical solitons) [16–20], from the works on dissipative solitons (mainly described by the generic cubic-quintic Ginzburg-Landau equation) [21–25], from the numerous results on ultrashort (few-cycle) optical solitons [26–31], and the works on optical rogue waves [32–35] and optical lattices [36–39]. The solitons supported by spin-orbit coupled BECs (see Ref. [40], also in this volume) have attracted substantial recent interest due to the novel features they exhibit (*e.g.*, *Zitterbewegung* oscillations). On this topic, let us mention that dark-dark solitons which occupy both energy bands of the spectrum of a spin-orbit coupled BEC have been recently shown to exist (see Ref. [41]) and that, interestingly enough, these solitonic structures are embedded families of bright, twisted or higher excited solitons inside a dark soliton, a configuration which is possible only within spin-orbit coupled BECs.

Outside of soliton-related research one finds a plethora of studies on various nonlinear features of BECs which go from chaotic dynamics and quantum turbulence (see, for example, Refs. [42–48]) to phase transitions and nonequilibrium phenomena (see the recent Refs.[49–52]), to name only a few topics of an otherwise very diverse research landscape.

Many of the aforementioned theoretical investigations into the properties of BECs rely on an accurate numerical treatment of the GPE, a practical problem which gradually developed into a research direction in its own rights. Among the early numerical methods used to obtain the ground state of trapped BECs we mention the explicit imaginary-time algorithm which is presented in Ref. [53], while for the dynamics of dynamics of the condensate we refer the reader to the explicit finite-difference scheme for the GPE presented in Ref. [54]. A popular numerical solution of the time-dependent GPE based on time-splitting spectral methods is discussed in Ref. [55]. A solution of a different type is presented in Ref. [56], where the GPE is solved by expanding the condensate wave function in terms of the solutions of the simple-harmonic oscillator which characterizes the magnetic trap. Ref. [57] shows the solution of the GPE using a symplectic shooting method, while Ref. [58] discusses in detail a package of Fotran codes which describe the stationary states and the nonlinear dynamics of one-, two- and three-dimensional BECs. Other popular methods used to solve the GPE through pseudospectral and finite-difference methods are detailed in Refs. [59–62]. While different with respect to the underlying

numerical method, all previous treatments of the GPE are intrinsically sequential and therefore time-consuming. The C codes in Ref. [63] are parallelized using the OpenMP approach such that the execution time decreases by almost one order of magnitude on a standard desktop computers with multi-core CPUs.

In the first part of this article, Sections 2 and 3, we present briefly the Gross-Pitaesvkii formalism and survey a series of results concerning the effective equations which describe the dynamics of elongated (cigar-shaped) and oblate (pancake-shaped) Bose-Einstein condensates. The second part of the paper, Section 4, details the construction of effective one- and two-dimensional polynomial Schrödinger equations which describe the longitudinal (transversal) dynamics of high-density cigar-shaped (pancake-shaped) Bose-Einstein condensates. Finally, Section 5 gathers our concluding remarks.

2. THE GROSS-PITAEVSKII FORMALISM

As at low energies the effective interaction between two bosons is a constant in the momentum representation, *i.e.*, $g = 4\pi\hbar^2 a_s/m$, where a_s is the s-wave scattering length and m is the mass of the boson, we have that the effective Hamiltonian for the condensed state is given by

$$\hat{\mathcal{H}} = \sum_{j=1}^{N} \left[\frac{\hat{\mathbf{p}}_j^2}{2m} + V(\mathbf{r}_j) \right] + g \sum_{j<n} \delta(\mathbf{r}_j - \mathbf{r}_n), \tag{1}$$

where $V(\mathbf{r})$ is the external potential and N is the number of bosons. For positive scattering lengths the effective interaction is repulsive, while for negative ones the effective interaction is attractive. In the following pages we will only address the case of repulsive interactions.

The energy of the condensed state is given by

$$\mathcal{E}(\phi) = N \int d\mathbf{r} \left[\frac{\hbar^2}{2m} |\nabla\phi(\mathbf{r})|^2 + V(r) |\phi(\mathbf{r})|^2 + \frac{N-1}{2} g |\phi(\mathbf{r})|^4 \right], \tag{2}$$

where $\phi(\mathbf{r})$ is the single-particle state. Above, we assumed that all atoms are in the same single-particle state whose wavefunction is ϕ. This relies on the Hartree-Fock approximation according to which we can write the many-body state as

$$\psi(\mathbf{r}_1,\dots,\mathbf{r}_N) = \prod_{j=1}^{N} \phi(\mathbf{r}_j). \tag{3}$$

Consequently, the energy functional equation (2), the so-called Gross-Pitaevskii energy functional, provides a mean field description of the condensate. We stress that

the $|\phi(\mathbf{r})|^4$ term of the Gross-Pitaevskii energy functional (hence the nonlinearity present in the Schrödinger-like equations to be derived below) comes from the inter-atomic interaction.

Instead of working with the single-particle state it is customary to work with the wavefunction of the condensate, or the order parameter as it is sometimes called, defined as $\psi(\mathbf{r}) = \sqrt{N}\phi(\mathbf{r})$. Therefore the density of bosons is given by $n(\mathbf{r}) = |\psi(\mathbf{r})|^2$ while equation (2) becomes

$$\mathcal{E}(\psi) = \int d\mathbf{r} \left[\frac{\hbar^2}{2m} |\nabla\psi(\mathbf{r})|^2 + V(r)|\psi(\mathbf{r})|^2 + \frac{g}{2}|\psi(\mathbf{r})|^4 \right],   \tag{4}$$

where we have used that $N - 1 \approx N$. The stationary states of the Bose-condensed gas are obtained from the requirement that

$$\frac{\partial \mathcal{G}}{\partial \psi^*} = 0,   \tag{5}$$

where $\mathcal{G} = \mathcal{E} - \mu N$. The Lagrange multiplier μ was introduced to assure the constant number of particles, and $\partial\mathcal{G}/\partial\psi^*$ represents the functional derivative of $\mathcal{G}$ with respect to ψ^* and yields

$$-\frac{\hbar^2}{2m}\nabla^2\psi(\mathbf{r}) + V(\mathbf{r})\psi(\mathbf{r}) + g\psi(\mathbf{r})|\psi(\mathbf{r})|^2 = \mu\psi(\mathbf{r}),   \tag{6}$$

which is the time-independent Gross-Pitaevskii equation. Its time-dependent sibling is given by

$$i\hbar\frac{\partial}{\partial t}\psi(\mathbf{r},t) = \left[-\frac{\hbar^2}{2m}\nabla^2 + V(\mathbf{r}) + g|\psi(\mathbf{r},t)|^2 \right]\psi(\mathbf{r},t),   \tag{7}$$

and describes the time evolution of the order parameter $\psi(\mathbf{r},t)$.

3. NON-POLYNOMIAL SCHRÖDINGER EQUATIONS

While the aforementioned theoretical efforts have been unfruitful for condensates with the long-range interactions, such as dipolar BECs, there are numerous results for condensates with short-range interactions where one can describe strongly elongated and strongly oblate condensates using effectively one- and two-dimensional equations, respectively (see Refs. [64–70] for an overview). The common feature of all these equations of reduced dimensionality is that they approximate analytically the radial or the transversal dynamics of the condensate such the resulting equation has a reduced dimensionality. This simplification comes at the cost of a non-polynomial resulting nonlinearity which precludes standard analytical solutions (such as solitons) and generally allows only for a limited analytical insight. One usu-

ally distinguishes between two qualitatively different density regimes: the low- and the high-density regime of BECs.

3.1. LOW-DENSITY CONDENSATES

For practical purposes, it is convenient to work with the three-dimensional GPE subject to the natural constraint that the wavefunction is normalized to unity, namely

$$i\hbar\frac{\partial}{\partial t}\psi\left(\mathbf{r},t\right) \;=\; \left[-\frac{\hbar^2}{2m}\nabla^2 + V\left(\mathbf{r}\right) + gN\left|\psi\left(\mathbf{r},t\right)\right|^2\right]\psi\left(\mathbf{r},t\right), \qquad (8)$$

where

$$\int d\mathbf{r}\left|\psi\left(\mathbf{r},t\right)\right|^2 = 1, \qquad (9)$$

and with the harmonic trapping potential

$$V(\mathbf{r}) \;=\; \frac{m}{2}\Omega_\perp^2\left(x^2+y^2\right) + \frac{m}{2}\Omega_z^2 z^2, \qquad (10)$$

$$=\; V(x,y) + V(z). \qquad (11)$$

One then computes the action

$$S \;=\; \int dt d\mathbf{r}\,\psi^*\left[i\hbar\frac{\partial}{\partial t} + \frac{\hbar^2}{2m}\nabla^2 - V\left(\mathbf{r}\right) - \frac{1}{2}gN\left|\psi\left(\mathbf{r},t\right)\right|^2\right]\psi \qquad (12)$$

for a convenient trial wavefunction and minimizes the ensuing functional with respect to the corresponding variational parameters. In the case of a cigar-shaped condensate, the trial wavefunction can be decomposed inro a radial and a longitudinal part as

$$\psi\left(\mathbf{r},t\right) \;=\; \phi\left(x,y,t;\sigma\left(z,t\right)\right)f\left(z,t\right), \qquad (13)$$

where

$$\phi\left(x,y,t;\sigma\left(z,t\right)\right) \;=\; \frac{\exp\left[\dfrac{-\left(x^2+y^2\right)}{2\sigma\left(z,t\right)^2}\right]}{\pi^{1/2}\sigma\left(z,t\right)}. \qquad (14)$$

We have chosen a Gaussian envelope for the radial component of the wavefunction because it allows us to compute the action without difficulty and reproduces the exact analytically known results in the limit of vanishing interaction $gN \to 0$. Our choice for the radial component of the wavefunction yields

$$S \;=\; \int dt dz\, f^*(z,t) \left[i\hbar \frac{\partial}{\partial t} + \frac{\hbar^2}{2m}\frac{\partial^2}{\partial z^2} - V(z) - \frac{1}{2}gN\frac{\sigma^{-2}}{2\pi}\left| f(z,t) \right|^2 \right.$$
$$\left. - \frac{\hbar^2}{2m}\sigma^{-2} - \frac{m\Omega_\perp^2}{2}\sigma^2 \right] f(z,t) \,. \tag{15}$$

Following the minimization with respect to f, f^* and σ, we arrive at an effectively one-dimensional partial-differential equation (and its complex conjugate)

$$i\hbar\frac{\partial}{\partial t}f(z,t) \;=\; \left[-\frac{\hbar^2}{2m}\frac{\partial^2}{\partial z^2} + V(z) + gN\frac{\sigma^{-2}}{2\pi}\left| f(z,t) \right|^2 \right.$$
$$\left. + \left(\frac{\hbar^2}{2m}\sigma^{-2} + \frac{m\omega_\perp^2}{2}\sigma^2 \right) \right] f(z,t) \,, \tag{16}$$

and one algebraic equation

$$\frac{\hbar^2}{2m}\sigma^{-3} - \frac{1}{2}m\Omega_\perp^2\sigma + \frac{1}{2}gN\frac{\sigma^{-3}}{2\pi}\left| f(z,t) \right|^2 \;=\; 0 \,, \tag{17}$$

which can be solved analytically. By doing so, we can reduce the partial-differential equation to

$$i\hbar\frac{\partial}{\partial t}f \;=\; \left[-\frac{\hbar}{2m}\frac{\partial^2}{\partial z^2} + V(z) + \frac{gNm\Omega_\perp}{2\pi\hbar}\frac{\left| f^2 \right|}{\sqrt{1+2a_sN\left| f \right|^2}} \right.$$
$$\left. + \frac{\hbar\Omega_\perp}{2}\left(\frac{1}{\sqrt{1+2a_sN\left| f \right|^2}} + \sqrt{1+2a_sN\left| f \right|^2} \right) \right] f \,, \tag{18}$$

where $f = f(z,t)$. Disregarding the longitudinal trapping of the condensate we can cast the previous equation in a very compact form, namely:

$$i\hbar\frac{\partial f}{\partial t} \;=\; \left[-\frac{\hbar}{2m}\frac{\partial^2}{\partial z^2} + \hbar\Omega_\perp\frac{1+3a_sN\left| f \right|^2}{\sqrt{1+2a_sN\left| f \right|^2}} \right] f \,, \tag{19}$$

which is widely used to describe the dynamics of low-density cigar-shaped condensates. The same variational treatment can be applied to pancake-shaped condensates, where one finds that the Euler-Lagrange equations yield two partial-differential equations, namely

$$i\hbar\frac{\partial}{\partial t}\phi = \left[-\frac{\hbar}{2m}\nabla_\perp^2 + V(x,y) + gN\frac{\eta^{-1}}{(2\pi)^{1/2}}|\phi|^2\right.$$
$$\left. + \left(\frac{\hbar^2}{2m}\eta^{-2} + \frac{m\omega_z^2}{2}\eta^2\right)\right]\phi, \tag{20}$$

as well as its complex conjugate (where ϕ is the radial component of the wavefunction), and the algebraic constraint

$$\frac{\hbar^2}{2m}\eta^{-3} - \frac{m\Omega_z^2}{2}\eta + gN\frac{\eta^{-2}}{2(2\pi)^{1/2}}|\phi|^2 = 0. \tag{21}$$

While the previous equation can be solved analytically (using the Ferrari-Cardano method for quartic equations), its exact solutions are not particularly insightful and one usually looks for simple approximations which match the features of the experimental setup under investigation. In the case of low-density condensates the previous equations yield

$$i\hbar\frac{\partial}{\partial t}\phi = \left[-\frac{\hbar}{2m}\nabla_\perp^2 + V(x,y) + \frac{gN(m\Omega_z)^{1/2}}{(2\pi)^{1/2}\hbar^{1/2}}|\phi|^2\right]\phi. \tag{22}$$

The previous equations have been introduced by Salasnich *et al.* in Ref. [64] and have been used in numerous computational investigations which are reviewed in Ref. [66].

3.2. HIGH-DENSITY CONDENSATES

For cigar-shaped high-density condensates one can use a *q*-Gaussian *Ansatz* for the radial component, namely

$$\psi(\mathbf{r},t) = \phi(\rho,t;a(z,t),q(z,t))f(z,t), \tag{23}$$

where $\rho = \sqrt{x^2+y^2}$,

$$\phi(\rho,t;a,q) = c\left(1-\rho^2 a(1-q)\right)^{1/(1-q)} \tag{24}$$

and

$$c = \sqrt{\frac{a(3-q)}{\pi}}, \tag{25}$$

such that wavefunction is properly normalized.

The *q*-Gaussian *Ansatz* provides an accurate description of the condensate in both the low- and high-density regime and has been initially used to describe the ground-state properties of trapped BECs (see Refs. [71–73] and references therein).

Following the same steps as above one arrives at

$$i\hbar\frac{\partial f}{\partial t} = \left\{-\frac{\hbar^2}{2m}\frac{\partial^2}{\partial z^2} + 2\hbar\omega_\perp\left[\sqrt{a_s|f|^2 N} - \frac{2^{1/3}}{3}\left(a_s|f|^2 N\right)^{1/6}\right]\right\}f\,,(26)$$

where, as before, $f = f(z,t)$. This last equation is the high-density counterpart of equation (18). A similar equation can be derived for an oblate condensate (see Ref. [69] for a detailed discussion), but the computations are not straightforward, as the action yields special functions which one has to approximate in order to arrive at a relatively simple effective equation.

The efficiency of this variational treatment depends strongly on the accuracy of the *Ansatz* used for the radial/transversal component of the wavefunction and one usually aims at balancing the analytic tractability of the spatial integration (which effectively reduces the dimensionality of the system) with the complexity of the *Ansatz*. Most such variational approaches yield clear partial differential equations, but in the context of binary condensates, *i.e.*, either mixtures of different Bose-Einstein-condensed atomic species or one single atomic Bose-Einstein-condensed atomic species in different hyperfine states, one is also faced with sets of algebraic-differential equations (see, for example, Ref. [74]). These sets of equations consist of algebraic and partial differential equations and amount to solving numerically a set of algebraic equations at each time-iteration of the partial-differential equations.

On a related topic, let us note here the work of Band *et al.* [75] who showed that one can provide a unified semiclassical approximation for BECs which amounts to a one-dimensional nonlinear Schrödinger equation subject to a noncanonical (quartic) normalization condition.

4. EFFECTIVE LOW-DIMENSIONAL POLYNOMIAL SCHRÖDINGER EQUATIONS

The effective equations or reduced dimensionality discussed in the previous section come at the cost of a significantly increased computing time which is due to their non-polynomial structure. Evaluating, for instance, the wavefunction to the power 1/6, which appears in the NPSE equation reported in equation (26), is almost one order of magnitude more time-expensive than computing the square of the wavefunction in the one-dimensional GPE. Moreover, the effective low-dimensional equations which stem from variational recipes based on q-Gaussian *Ansätze* usually involve special functions which add an extra load to the computing time. Naturally, the numerical solution of NPSE is less time-consuming than that of the fully three-dimensional GPE, but for detailed numerical investigations their efficiency is insufficient to address some of the current research problems such as the dynamics of vortices in pancake-shaped condensates (see, *e.g.*, Ref. [76]).

In the case of a cigar-shaped condensate one solution to this problem is to integrate directly the radial component of the wavefunction in the GPE and solve numerically the resulting partial-differential equation. To this end, one needs a relatively simple analytical approximation for the radial component of the wavefunction which is amenable to symbolic integration. The Gaussians are the ideal choice in terms of tractability of the symbolic integration, but they fail to describe quantitatively high-density condensates. However, the previously mentioned q-Gaussian functions can be used to construct *Ansätze* which are exact solutions to the GPE in both the low- and the high-density regime, but the variational parameters come only in a numerical form from the solution of a set of nonlinear algebraic equations which (unlike equation (17)) do not have exact analytic solutions. Considering a trial wavefunction of the form

$$\psi(\rho, z) = A \left(1 - \frac{(1 - q_r)\rho^2}{2w_r^2}\right)^{1/(1-q_r)} \left(1 - \frac{(1 - q_z)z^2}{2w_z^2}\right)^{1/(1-q_z)}, \qquad (27)$$

where A is chosen such that the wavefunction is normalized to unity, we have the following variational equations

$$
\begin{aligned}
5\sqrt{2}gmN (q_r - 3)^2 (q_r - 2)(q_r + 1)(25q_z - 126) + \\
3528\pi (q_r - 5) w_z \left(m^2 (q_r + 1) w_r^4 \Omega_\perp^2 - (q_r - 3)(q_r - 2)\hbar^2\right) &= 0, \quad (28) \\
5\sqrt{2}gmN (q_r - 3)^2 (1 + q_z)(3q_z - 7)(25q_z - 126) w_z + \\
1764\pi (q_r - 5) w_r^2 \left(8m^2 (1 + q_z) w_z^4 \Omega_z^2 - (q_z - 5)(3q_z - 7)\hbar^2\right) &= 0, \quad (29) \\
5\sqrt{2}gmN (q_r - 7)(q_r - 3)\left(2 + q_r - q_r^2\right)^2 (25q_z - 126) + \\
3528\pi (q_r - 5)^2 w_z \left(m^2 (1 + q_r)^2 w_r^4 \Omega_\perp^2 - 4(q_r - 2)^2 \hbar^2\right) &= 0, \quad (30) \\
125\sqrt{2}gmN (q_r - 3)^2 \left(7 + (4 - 3q_z)q_z\right)^2 w_z + \\
5292\pi (q_r - 5) w_r^2 \left(4m^2 (1 + q_z)^2 w_z^4 \Omega_z^2 - (7 - 3q_z)^2 \hbar^2\right) &= 0, \quad (31)
\end{aligned}
$$

where w_z and w_r are the longitudinal and the radial width of the condensate and q_z and q_r are the q-parameters which show how deep in the Thomas-Fermi regime the condensate is. Figures 1 and 2 show the accuracy of the above variational treatment for the high-density cigar- and pancake-shaped ^{87}Rb condensate of $N = 10^8$ atoms.

The results in Figure 1 correspond to a cigar-shaped condensate loaded into a standard magnetic trap with frequencies $\Omega_\perp = 160 \times 2\pi$ Hz and $\Omega_z = 7 \times 2\pi$ Hz, while those in Figure 2 address a pancake-shaped condensate loaded in a trap with frequencies $\Omega_z = 160 \times 2\pi$ Hz and $\Omega_\perp = 7 \times 2\pi$ Hz. In both cases the variational results capture accurately the spatial extent of the condensate on the radial and on the longitudinal axes and the peak density, but exhibit a somewhat "edgy" appearance
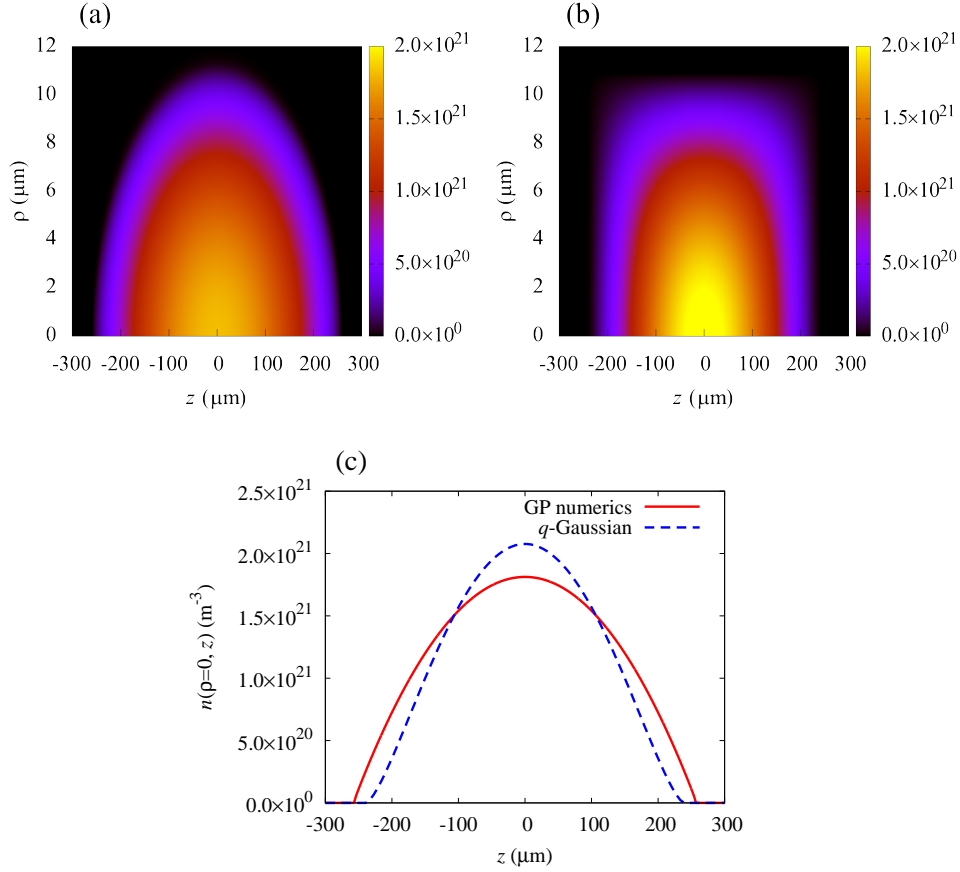
Fig. 1 – Ground-state density profile of a ^{87}Rb cigar-shaped condensate of $N = 10^8$ atoms. The frequencies of the magnetic trap are $\Omega_\perp = 160 \times 2\pi$ Hz and $\Omega_z = 7 \times 2\pi$ Hz. Panel (a) depicts the $\rho - z$ density plot of the ground-state profile $n(\rho, z) = |\psi(\rho, z)|^2$ obtained by the full GPE imaginary-time numerics [78, 79], while panel (b) shows the corresponding results of the variational equations (28)-(31). Panel (c) gives a comparison of the two results for a BEC density at the longitudinal axis. Please note that the variational results capture accurately the bulk properties of the density profile (spatial extent along the ρ and z axes, peak density, etc.). The somewhat "edgy" appearance of the density profile in panel (b) obtained from the variational equations is due to the zeros of the wavefunction of the condensate, which decays exponentially to zero only in the $q \to 1$ limit.

due to the zeros of the wavefunction of the condensate, which decays exponentially to zero only in the $q \to 1$ limit (*i.e.*, in the low-density regime). Equations (28)-(31) generalize the one-dimensional variational calculations reported in Ref. [77] and reproduce the Thomas-Fermi results for high-density condensates (*i.e.*, in the $q \to -1$ limit). We point out, however, that for all values of $q \neq -1$ our variational *Ansatz*
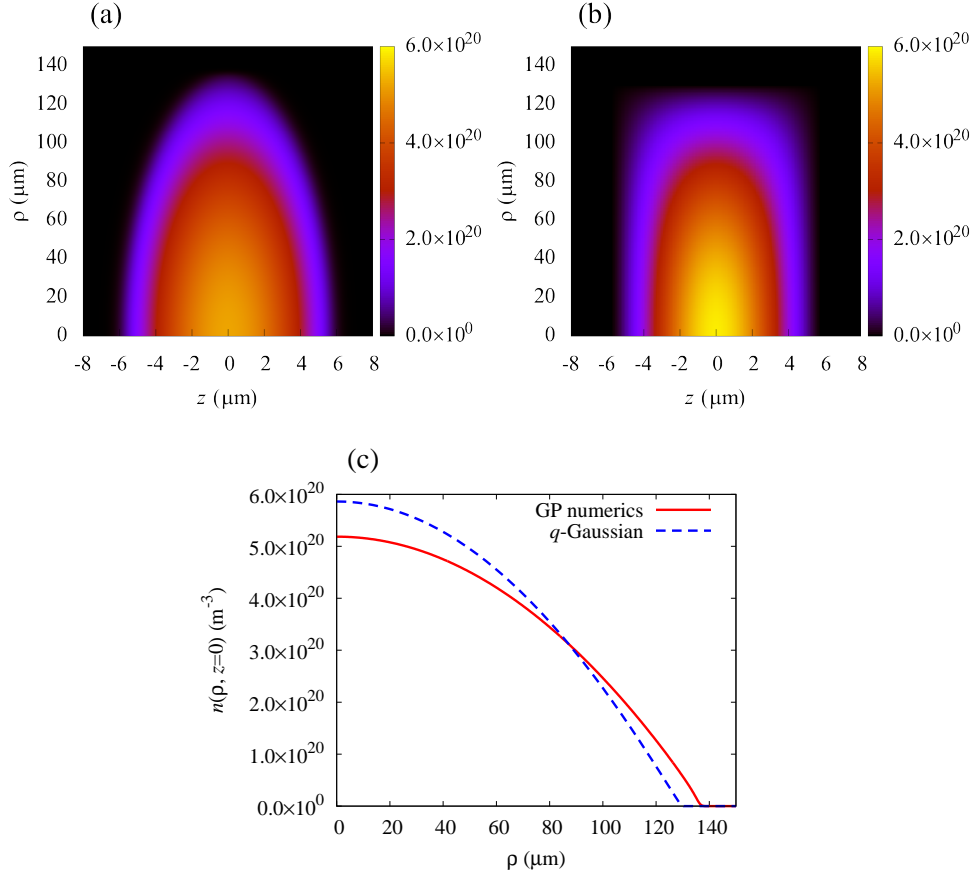
Fig. 2 – Ground-state density profile of a ^{87}Rb pancake-shaped condensate of $N = 10^8$ atoms. The frequencies of the magnetic trap are $\Omega_z = 160 \times 2\pi$ Hz and $\Omega_\perp = 7 \times 2\pi$ Hz. As before, panel (a) depicts the $\rho - z$ density plot of the ground-state profile $n(\rho, z) = |\psi(\rho, z)|^2$ obtained by the full GPE imaginary-time numerics [78, 79], while panel (b) shows the corresponding results of the variational equations (28)-(31). Panel (c) gives a comparison of the two results for a BEC density in the radial direction. The variational results capture accurately the bulk properties of the density profile (spatial extent along the ρ and z axes, peak density, etc.). The somewhat "edgy" appearance of the density profile in panel (b) is due to the zeros of the wavefunction, which does not decay exponentially to zero.

allows for a straightforward calculation of the kinetic energy term of the condensate due to the q-Gaussian tail which avoids the singularity exhibited by the standard Thomas-Fermi approximation. This, in turn, allows us to integrate directly on the GPE either the longitudinal or the transversal component of the wavefunction and derive an effective one- or two-dimensional equation with cubic nonlinearity for the radial or transversal component of the wavefunction of the condensate. Naturally, the

ensuing effective equations of low dimensionality are easier to solve numerically and allow for straightforward analytical insight (see, *e.g.*, the discussion on the effectively linear dynamics of collisionally inhomogeneous condensates in Ref. [80]).

Detailed calculations which will be reported elsewhere show that for a strongly elongated condensate of high density (*i.e.*, in the $q \to -1$ limit) with cylindrical symmetry, the three-dimensional GPE reduces to a one-dimensional GPE with rescaled coefficients, namely

$$
i\frac{2}{3}\sqrt{2\pi}w_r\hbar\frac{\partial f}{\partial t} = -\frac{\sqrt{2\pi}w_r\hbar^2}{3m}\frac{\partial^2 f}{\partial z^2} + \frac{2}{15}m\sqrt{2\pi}w_r^3\Omega_\perp^2 f + \frac{1}{3}m\sqrt{2\pi}w_r z^2\Omega_z^2 f
$$
$$
+ \frac{4g}{5w_r}\sqrt{\frac{2}{\pi}}|f|^2 f\,, \tag{32}
$$

where w_r is obtained from the numerical solution of equations (28)-(31). To arrive at equation (32) we integrate out the radial component of the wavefunction in equation (7) considering that

$$
\psi(\rho,z) = f(z,t)B\left(1 - \frac{(1-q_r)\rho^2}{2w_r^2}\right)^{1/(1-q_r)}\,, \tag{33}
$$

where B is chosen such that the radial component of the wavefunction is normalized to unity and linearize the ensuing equation around $q_r = -1$. To determine numerically the value of w_r we use equations (28)-(31). Similarly, for a strongly oblate condensate we arrive at

$$
i\frac{\sqrt{3}}{4}\pi\sqrt{w_z}\hbar\frac{\partial \phi}{\partial t} = -\frac{\sqrt{3}\pi\sqrt{w_z}h^2}{8m}\nabla_\perp^2\phi + \frac{\sqrt{3}}{8}m\pi\sqrt{w_z}\left(x^2 + y^2\right)\Omega_\perp^2\phi
$$
$$
+ \frac{\sqrt{3}}{32}m\pi w_z^{5/2}\Omega_z^2\phi + \frac{9\sqrt{3}g\pi}{64\sqrt{w_z}}|\phi|^2\phi\,, \tag{34}
$$

where w_z is obtained from the numerical solutions of equations (28)-(31) and we consider a wave wavefunction of the form

$$
\psi(x,y,z) = \phi(x,y,t)A\left(1 - \frac{(1-q_z)z^2}{2w_z^2}\right)\,, \tag{35}
$$

with A such that the transverse component of the wavefunction is normalized to unity.

Unlike the equations discussed in the previous section, equations (32) and (34) do not capture the interplay between the radial and the transversal modes, but can capture accurately the dynamics of effectively longitudinal or transverse nonlinear waveforms through their rescaled effective nonlinearities, for instance, the collision between two solitons in a cigar-shaped condensate, or the dynamics of vortices in a pancake-shaped condensate (the latter being extremely relevant for the experimental results reported in Ref. [76]).

5. CONCLUSIONS

The first part of the paper was devoted to an overview of the BEC fundamentals and to a brief survey of the variational methods which allow effective one- and two-dimensional dimensional descriptions of elongated and oblate three-dimensional condensates. We point out that the reduced dimensionality comes at the cost of a non-polynomial structure of the final effective equations, which is detrimental both to the numerical and analytical computations. In the second part of the paper we have shown that under the assumption that the radial (transversal) component of the wavefunction remains in its ground state one can obtain an effective one-dimensional (two-dimensional) polynomial Schrödinger equation for the longitudinal (transversal) dynamics. To this end, we have used a q-Gaussian *Ansatz* for the radial (transversal) part of the wavefunction and have considered that the number of atoms is high enough, such that the condensate is well in the Thomas-Fermi regime. Our equations do not capture the interplay between the radial and the transversal modes of the condensate, but can provide a quantitative description of the dynamics of longitudinal nonlinear waveforms in cigar-shaped condensates and that of transversal nonlinear waveforms in pancake-shaped BECs.

REFERENCES

1. C. J. Pethick and H. Smith, *Bose-Einstein condensation in dilute gases* (Cambridge University Press, Cambridge, 2008).
2. L. P. Pitaevskii and S. Stringari, *Bose-Einstein Condensation* (Clarendon Press, Oxford, 2003).
3. J. T. Mendonca and H. Tercas, *Physics of Ultra-Cold Matter. Atomic Clouds, Bose-Einstein Condensates and Rydberg Plasmas* (Springer, New York, 2014).
4. F. Dalfovo, S. Giorgini, L. P. Pitaevskii, and S. Stringari, Rev. Mod. Phys. **71**, 463 (1999).
5. E. A. Cornell and C. E. Wieman, Rev. Mod. Phys. **74**, 875 (2002).
6. W. Ketterle, Rev. Mod. Phys. **74**, 1131 (2002).
7. A. L. Legget, Rev. Mod. Phys. **73**, 307 (2003).
8. V. S. Bagnato, D. J. Frantzeskakis, P. G. Kevrekidis, B. A. Malomed, and D. Mihalache, Rom. Rep. Phys. **67**, 5 (2015).
9. R. Radha and P. S. Vinayagam, Rom. Rep. Phys. **67**, 89 (2015).
10. E. P. Gross, Nuovo Cim. **20**, 454 (1961).

11. L. P. Pitaevskii, Zh. Eksp. Teor. Fiz. **40**, 646 (1961).

12. C. Sulem and P.-L. Sulem, *The nonlinear Schrödinger equation* (Springer, New York, 1999).

13. P. G. Kevrekidis, D. J. Frantzeskakis, R. Carretero-González, and I. G. Kevrekidis, Mod. Phys. Lett. B **18**, 1481 (2004).

14. F. Kh. Abdullaev, A. Gammal, A. M. Kamchatnov, and L. Tomio, Int. J. Mod. Phys. B **19**, 3415 (2005).

15. D. J. Frantzeskakis, J. Phys. A: Math. Theor. **43**, 213001 (2010).

16. B. A. Malomed, D. Mihalache, F. Wise, and L. Torner, J. Opt. B: Quantum Semiclassical Opt. **7**, R53 (2005).

17. Y. V. Kartashov, B. A. Malomed, and L. Torner, Rev. Mod. Phys. **83**, 247 (2011).

18. Z. G. Chen, M. Segev, and D. N. Christodoulides, Rep. Prog. Phys. **75**, 086401 (2012).

19. D. Mihalache, Rom. J. Phys. **57**, 352 (2012).

20. D. Mihalache, Rom. J. Phys. **59**, 295 (2014).

21. L. C. Crasovan, B. A. Malomed, and D. Mihalache, Phys. Rev. E **63**, 016605 (2001).

22. P. Grelu and N. Akhmediev, Nature Photon. **6**, 84 (2012).

23. R. J. Li, P. F. Li, and L. Li, Proc. Romanian Acad. A **14**, 121 (2013).

24. V. Skarka *et al.*, Phys. Rev. A **90**, 023845 (2014).

25. Y. J. He, B. A. Malomed, and D. Mihalache, Phil. Trans. R. Soc. A **372**, 20140017 (2014).

26. I. V. Melnikov, D. Mihalache, F. Moldoveanu, and N.-C. Panoiu, Phys. Rev. A **56**, 1569 (1997).

27. S. V. Sazonov and A. F. Sobolevskii, JETP **96**, 1019 (2003).

28. S. V. Sazonov, Bull. Russian Acad. Sciences **75**, 157 (2011).

29. H. Leblond and D. Mihalache, Phys. Rep. **523**, 61 (2013).

30. H. Leblond, H. Triki, and D. Mihalache, Rom. Rep. Phys. **65**, 925 (2013).

31. D. J. Frantzeskakis, H. Leblond, and D. Mihalache, Rom. J. Phys. **59**, 767 (2014).

32. D. R. Solli, C. Ropers, P. Koonath, and B. Jalali, Nature (London) **450**, 1054 (2007).

33. N. Akhmediev, J. M. Dudley, D. R. Solli, and S. K. Turitsyn, J. Opt. **15**, 060201 (2013).

34. G. Y. Yang, L. Li, S. T. Jia, and D. Mihalache, Rom. Rep. Phys. **65**, 391 (2013).

35. G. Y. Yang, L. Li, S. T. Jia, and D. Mihalache, Rom. Rep. Phys. **65**, 902 (2013).

36. T. D. Grass, F. E. A. dos Santos, and A. Pelster, Phys. Rev. A **84**, 013613 (2011).

37. M. Mobarak and A. Pelster, Laser Phys. Lett. **10**, 115501 (2013).

38. T. Wang, X.-F. Zhang, S. Eggert, and A. Pelster, Phys. Rev. A **87**, 063615 (2013).

39. T. Wang, X.-F. Zhang, F. E. A. dos Santos, S. Eggert, and A. Pelster, Phys. Rev. A **90**, 013633 (2014).

40. V. Achilleos, D. J. Frantzeskakis, P. G. Kevrekidis, P. Schmelcher, and J. Stockhofe, Rom. Rep. Phys. **67**, 235 (2015).

41. V. Achilleos, D. J. Frantzeskakis, and P. G. Kevrekidis, Phys. Rev. A **89**, 033636 (2014).

42. M. Diver, G. R. M. Robb, and G.-L. Oppo, Phys. Rev. A **89**, 033602 (2014).

43. E. A. L. Henn, J. A. Seman, G. Roati, K. M. F. Magalhes, and V. S. Bagnato, Phys. Rev. Lett. **103**, 045301 (2009).

44. V. S. Bagnato *et al.*, *Characteristics and Perspectives of Quantum Turbulence in Atomic Bose-Einstein Condensates*, in *Physics of Quantum Fluids. New Trends and Hot Topics in Atomic and Polariton Condensates*, pp. 301-314, edited by Alberto Bramati and Michele Modugno (Springer, New York, 2013).

45. J. A. Seman *et al.*, Journal of Physics: Conference Series **264**, 012004 (2011).

46. B. Villasenor, R. Zamora-Zamora, D. Bernal, and V. Romero-Rochin, Phys. Rev. A **89**, 033611 (2014).

47. M. A. Caracanhas, E. A. L. Henn, and V. S. Bagnato, Rom. Rep. Phys. **67**, 51 (2015).
48. A. Vardi, Rom. Rep. Phys. **67**, 67 (2015).
49. C. Hamner, C. Qu, Y. Zhang, J. J. Chang, M. Gong, C. Zhang, and P. Engels, Nature Communications **5**, 4023 (2014).
50. E. Witkowska, T. Swislocki, and M. Matuszewski, Phys. Rev. A **90**, 033604 (2014).
51. H.-S. Tao, W. Wu, Y.-H. Chen, and W.-M. Liu, Rom. Rep. Phys. **67**, 187 (2015).
52. V. I. Yukalov and E. P. Yukalova, Rom. Rep. Phys. **67**, 159 (2015).
53. M. M. Cerimele, M. L. Chiofalo, F. Pistella, S. Succi, and M. P. Tosi, Phys. Rev. E **62**, 1382 (2000).
54. M. L. Chiofala, S. Succi, and M. P. Tosi, Phys. Rev. E **62**, 7438 (2000).
55. W. Bao, D. Jaksch, and P. A. Markowich, J. Comput. Phys. **187**, 318 (2003).
56. R. P. Tiwari and A. Shukla, Comput. Phys. Commun. **174**, 966 (2006).
57. W. Hua, X. Liu, and P. Ding, J. Math. Chem. **40**, 243 (2006).
58. P. Muruganandam and S. K. Adhikari, Comput. Phys. Commun. **180**, 1888 (2009).
59. S. K. Adhikari, Phys. Lett. A **265**, 91 (2000).
60. S. K. Adhikari, Phys. Rev. E **62**, 2937 (2000).
61. S. K. Adhikari and P. Muruganandam, J. Phys. B: At. Mol. Opt. Phys. **35**, 2831 (2002).
62. P. Muruganandam and S. K. Adhikari, J. Phys. B: At. Mol. Opt. Phys. **36**, 2501 (2003).
63. D. Vudragović, I. Vidanović, A. Balaž, P. Muruganandam, and S. K Adhikari, Comput. Phys. Commun. **183**, 2021 (2012).
64. L. Salasnich, A. Parola, and L. Reatto, Phys. Rev. A **65**, 043614 (2002).
65. L. Salasnich, Laser Phys. **12**, 198 (2002).
66. L. Salasnich, J. Phys. A: Math. Theor. **42**, 335205 (2009).
67. A. Muñoz Mateo and V. Delgado, Phys. Rev. A **77**, 013607 (2008).
68. A. Muñoz Mateo and V. Delgado, Ann. Phys. **324**, 709 (2009).
69. A. I. Nicolin, Rom. Rep. Phys. **61**, 641 (2009).
70. A. I. Nicolin and M. C. Raportaru, Physica A **389**, 4663 (2010).
71. A. L. Fetter, J. Low. Temp. Phys. **106**, 643 (1997).
72. K. S. Fa, R. S. Mendes, P. R. B. Pedreira, and E. K. Lenzi, Physica A **295**, 242 (2001).
73. E. Erdemir and B. Tanatar, Physica A **322**, 449 (2003).
74. S. Middelkamp, J. J. Chang, C. Hamner, R. Carretero-González, P. G. Kevrekidis, V. Achilleos, D. J. Frantzeskakis, P. Schmelcher, and P. Engels, Phys. Lett. A **375**, 642 (2011).
75. Y. B. Band, I. Towers, and B. A. Malomed, Phys. Rev. A **67**, 023602 (2003).
76. R. Navarro, R. Carretero-González, P. J. Torres, P. G. Kevrekidis, D. J. Frantzeskakis, M. W. Ray, E. Altuntas, and D S. Hall, Phys. Rev. Lett. **110**, 225301 (2013).
77. A. I. Nicolin and R. Carretero-González, Physica A **387**, 6032 (2008).
78. P. Muruganandam and S. K. Adhikari, Comput. Phys. Commun. **180**, 1888 (2009).
79. D. Vudragović, I. Vidanović, A. Balaž, P. Muruganandam, and S. K. Adhikari, Comput. Phys. Commun. **183**, 2021 (2012).
80. A. Balaž, R. Paun, A. I. Nicolin, S. Balasubramanian, and R. Ramaswamy, Phys. Rev. A **89**, 023609 (2014).